

Article

Combined Chemical Modification of Bamboo Material Prepared Using Vinyl Acetate and Methyl Methacrylate: Dimensional Stability, Chemical Structure, and Dynamic Mechanical Properties

Saisai Huang ¹, Qiufang Jiang ¹, Bin Yu ², Yujing Nie ¹, Zhongqing Ma ^{1,*}  and Lingfei Ma ^{1,*}

¹ School of Engineering, Zhejiang Provincial Collaborative Innovation Center for Bamboo Resources and High-Efficiency Utilization, Zhejiang A & F University, Hangzhou 311300, China

² Huzhou Ruiyi Wood Industry Co., Ltd., Huzhou 313220, China

* Correspondence: mazqzafu@163.com (Z.M.); malingfei@zafu.edu.cn (L.M.);

Tel.: +86-571-6110-0905 (Z.M. & L.M.)

Received: 24 August 2019; Accepted: 8 October 2019; Published: 11 October 2019



Abstract: Acetylation and in situ polymerization are two typical chemical modifications that are used to improve the dimensional stability of bamboo. In this work, the combination of chemical modification of vinyl acetate (VA) acetylation and methyl methacrylate (MMA) in situ polymerization of bamboo was employed. Performances of the treated bamboo were evaluated in terms of dimensional stability, wettability, thermal stability, chemical structure, and dynamic mechanical properties. Results show that the performances (dimensional stability, thermal stability, and wettability) of bamboo that was prepared via the combined pretreatment of VA and MMA (VA/MMA-B) were better than those of raw bamboo, VA single-treated bamboo (VA-B), and MMA single-treated bamboo (MMA-B). According to scanning electron microscopy (SEM) and Fourier transform infrared spectroscopy (FTIR) analyses, VA and MMA were mainly grafted onto the surface of the cell wall or in the bamboo cell lumen. The antismoothing efficiency and contact angle of VA/MMA-B increased to maximum values of 40.71% and 107.1°, respectively. From thermogravimetric analysis (TG/DTG curves), the highest onset decomposition temperature (277 °C) was observed in VA/MMA-B. From DMA analysis, the storage modulus (E') of VA/MMA-B increased sharply from 15,057 Pa (untreated bamboo) to 17,909 Pa (single-treated bamboo), and the glass transition temperature was improved from 180 °C (raw bamboo) to 205 °C (single-treated bamboo).

Keywords: bamboo; chemical modification; dimensional stability; dynamic thermodynamic; acetic anhydride; methyl methacrylate

1. Introduction

Bamboo is an important fast-growing and renewable material, and has been widely used as raw material to produce bamboo flooring, bamboo wood composite, bamboo building templates, and bamboo decorative materials because of its high mechanical properties and low strength-to-weight ratio [1,2]. However, bamboo use is highly limited by its strong hygroscopicity; specifically, the free hydroxyl groups from bamboo cell walls result in poor dimensional stability. Currently, many physical or chemical modification methods, such as heat treatment [3–6], in situ polymerization with organic monomers [7–9], acetylation treatment [10–13], and modification with 1,3-dimethylol-4,5-dihydroxyethyleneurea (DMDHEU) [14–16], have been used to improve its poor dimensional stability.

Acetylation is a conventional chemical modification method in which acetyl groups ($\text{CH}_3\text{CO}-$) react with hydroxyl groups ($-\text{OH}$) linked to the cellulose of wood/bamboo material; therefore,

it improves the dimensional stability of bamboo [12,13,17–24]. The traditional reagents used in wood/bamboo acetylation modification are acetic anhydride (AA), acetyl chlorides (AC), and thioacetic acid (TA) [12,13]. However, acetylation pretreated with these reagents produces a large amount of byproducts of strong acid, and this causes undesirable odors, strength loss, and corrosion of metal fasteners [25,26].

Recently, vinyl acetate (VA) was developed as an environmentally friendly reagent used in acetylation modification [23,27–30]. The byproduct produced from VA acetylation is acetaldehyde, which has a low boiling point and is easily removed. Several researchers have reported that the dimensional stability of wood treated via VA acetylation was much better than that of AA-treated wood. For example, Jebrane et al. reported that the weight percentage gain (WPG) of maritime pine after VA acetylation was 26.2%, which was higher than that of AA-treated wood (20.5%). Additionally, the swelling of blocks treated with VA, which have a WPG above 20%, was always less puffed than AA-treated wood [23]. Furthermore, it has been reported that the bonding strength between VA and cellulose is better than that between AA and cellulose, and this results in a lower swelling coefficient [29]. More VA than AA enters into the voids of cell walls, thereby decreasing the volume of voids and limiting the overall swelling of samples [28,30].

In situ polymerization of unsaturated polymer monomers (e.g., methyl methacrylate (MMA), styrene, acrylonitrile, and acrylamide) within wood pores (e.g., vessels, tracheids, capillaries, and ray cells) to fabricate wood polymer composites (WPCs) is another effective modification method for strengthening the mechanical properties of wood or for protecting the wood matrix from being attacked by water or microorganisms [31–35]. Methyl methacrylate (MMA) is one of the most important vinyl monomers used in WPCs because it has low viscosity and is relatively inexpensive [36–40]. Matto et al. reported that pinewood samples treated via in situ polymerization of MMA resulted in a higher retention of monomers and densification, less variation of permanent swelling, and higher mechanical resistance [37]. Fu et al. grafted MMA onto a wood surface using the atom transfer radical polymerization (ATRP) method, which resulted in the wood having better hydrophobicity [39]. Shang et al. found that the macromechanical properties (bending modulus and compressive modulus) of rattan were highly improved when MMA was grafted onto the surface of rattan [38].

As previously stated, studies reported in the literature have mainly focused individually on VA acetylation or MMA in situ polymerization of wood [23,27,32,37,39,41,42]. These two methods have been documented, and it has been concluded that both lead, to different extents, to improved dimensional stability and increased decay resistance of wood. However, the combined use of these two methods with respect to the enhancement of bamboo properties has not been reported. In this study, the effects of chemical modification via single use of VA and MMA on dimensional stability, chemical properties, and thermodynamic properties of bamboo were investigated. Then, a combined chemical modification method of VA acetylation and MMA in situ polymerization was employed to achieve a synergistic improvement in the dimensional stability and mechanical properties of bamboo.

2. Materials and Methods

2.1. Materials

Bamboo, purchased from Huzhou Ruiyi Wood Industry Co., Ltd. (Huzhou, China), was cut into samples with dimensions of 20 mm × 20 mm × 5 mm (L × W × H, respectively, for dimensional stability analysis) and 35 mm × 12 mm × 2.5 mm (L × W × H, respectively, for dynamic thermodynamic analysis). Samples were oven-dried at 105 °C for 12 h until constant weight was obtained. The sizes and weights of each specimen were then measured to calculate the volume (V_0) and weight (W_0).

2.2. Bamboo Acetylation Pretreatment

Vinyl acetate (VA) acetylation pretreatment of bamboo was carried out in a stainless steel container equipped with a vacuum pump, pressure pump, and calcium chloride drying tube (Figure 1). First, the

bamboo specimen and vinyl acetate/dimethylformamide solution (1:1 V/V) with 0.5% concentration of potassium carbonate as the catalyst were added to the container. The container was then put under vacuum to -0.09 MPa, and this was maintained for 12 h. The container was then put into an oven and heated to 110 °C, which was maintained for 6 h. Finally, the acetylated samples were soaked in flowing water for 48 h to remove unreacted reagents and byproducts; then, the samples were dried in a vacuum oven under 0.01 MPa at 105 °C until a constant weight was obtained. The weight percentage gain (WPG) and the volume bulking efficiency (VBE) were calculated using Equations (1) and (2), respectively.

$$WPG = \frac{W_1 - W_0}{W_0} \quad (1)$$

$$VBE = \frac{V_1 - V_0}{V_0} \quad (2)$$

where W_1 and V_1 are respectively the absolute dry mass and volume of the samples before acetylation, and W_2 and V_2 are respectively the absolute dry mass and volume of the samples after acetylation.

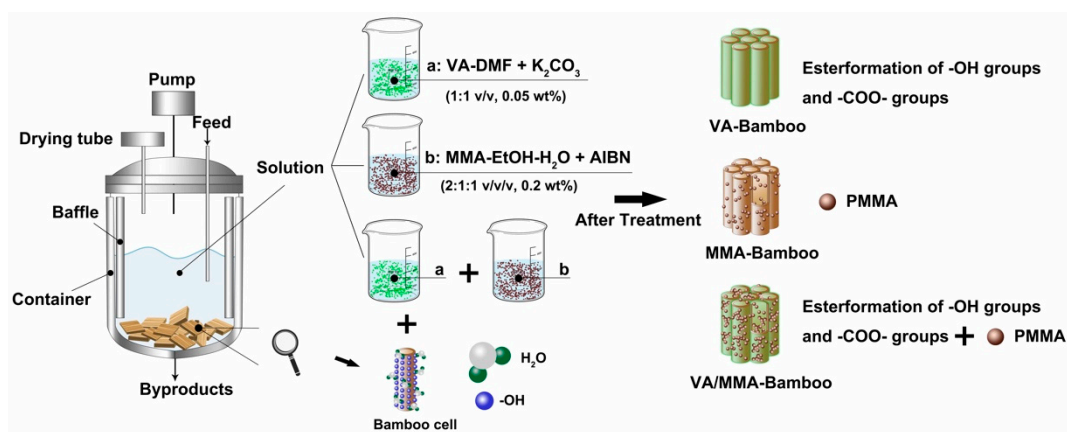


Figure 1. Schematic flow chart of bamboo acetylation, in situ polymerization of MMA on bamboo, and combined treatment of acetylation and in situ polymerization.

2.3. In Situ Polymerization of MMA on Bamboo

In situ polymerization of bamboo–MMA composite was carried out in the same container as mentioned above (Figure 1). First, MMA–EtOH solution (which was composed of MMA, ethanol, and deionized water with a volume ratio of 2:1:1) was added to the container. Azobisisobutyronitrile (AIBN), which is an initiator with a relative molar ratio of 1:5, was then also added to the container. Next, under vacuum/pressure cycles for 12 h, VA-acetylated samples and untreated samples were impregnated with the MMA–EtOH solution in the container. All of the samples were then washed to remove the residual solvent. Finally, the samples were wrapped in aluminum foil and stored for 24 h; samples were placed separately into the oven at 80 °C for 6 h. In the end, the VA/MMA-treated bamboo and MMA-treated bamboo were vacuum-dried under 0.01 MPa at 105 °C to obtain constant weight. The conversion rate (CR) of MMA was calculated using Equation (3):

$$CR = \frac{W_3 - W_0}{W_2 - W_0} \quad (3)$$

where W_3 is the oven-dried weight after polymerization, W_2 is the wet weight of bamboo after polymerization, and W_0 is the absolute dry mass and volume of bamboo before all of the treatments.

2.4. Characterization of Raw and Pretreated Bamboo

The surface functional groups of raw and pretreated bamboo were tested using Fourier transform infrared spectroscopy (FTIR, Nicolet Is50, Thermo Fisher Scientific, Waltham, MA, USA). The surface

morphologies of raw and pretreated bamboo were characterized using cold field emission scanning electron microscopy (SEM, SU8010, Hitachi, Chiyoda, Japan). The contact angles of raw and pretreated bamboo were measured using an interfacial tension tester (OCA200, DataPhysics, Filderstadt, Germany). The apparent contact angle was measured each second for the 5 s deposition on the surface of the sample. The thermal stabilities of raw and pretreated bamboo were tested using a thermogravimetric analyzer (TG-209, NETZSCH, Selb, Germany).

2.5. Dimensional Stability Analysis of Raw and Pretreated Bamboo

The dimensional stabilities of samples were evaluated using 12 specimens that were soaked in water for cyclic soaking–drying. Water soaking (at room temperature and under ambient pressure for 72 h) and oven-drying (103 °C for 24 h) were repeated three times. The weights and volumes of each sample were measured every cycle. Furthermore, the parameters of water absorption (WA), volume swelling efficiency (S_w), volume shrinking efficiency (S_k), and antishwelling efficiency (ASE) were calculated using Equations (4)–(7), respectively.

$$WA = \frac{W_{wi} - W_{w0}}{W_{w0}} \times 100\% \quad (4)$$

$$S_w = \frac{V_{wi} - V_{w0}}{V_{w0}} \times 100\% \quad (5)$$

$$S_k = \frac{V_{w0} - V_{wi}}{V_{wi}} \times 100\% \quad (6)$$

$$ASE = \frac{S_{wn} - S'_{wn}}{S'_{wn}} \times 100\% \quad (7)$$

where W_{wi} and V_{wi} are respectively the weight and size of a bamboo block after soaking it i times, and W_{w0} and V_{w0} are respectively the weight and size of a bamboo block after drying it i times. i is 1, 2, and 3. S_{wn} is the swelling efficiency of untreated bamboo, and S'_{wn} is that of reacted bamboo.

2.6. Dynamic Mechanical Analysis of Raw and Pretreated Bamboo

The storage modulus (E'), loss modulus (E''), and tan delta ($\tan \delta$) of both the raw and pretreated bamboo were recorded using a dynamic mechanical analyzer (DMA, Q800, TA Instruments, New Castle, DE, USA). The temperature was scanned from 40 to 240 °C, the heating rate was 2 °C/min, the frequency of the measurements was 1 Hz. Duplicate samples were measured to ensure the reproducibility of results.

3. Results

3.1. Weight Gain Rate, Volume Bulking Efficiency, and Conversion Rate

Table 1 shows the effects of using different modification methods on the weight gain rate (WPG) of bamboo, volume bulking efficiency (VBE) of bamboo, and conversion rate (CR) of MMA. WPG reached a maximum of 18.95% after the combined treatment of VA and MMA, and this indicates that more VA and MMA were fabricated on the bamboo. During the VA and MMA treatment process, VA has an active anhydride group that reacts with hydroxyl groups of bamboo components to create monoesters [28,29], and MMA in situ polymerizes on the surface or in a void of bamboo [23]. Ghorbani et al. reported that the WPG of poplar wood increased from 22.71% with the single treatment of maleic anhydride (MAN) and from 51.8% with the single treatment of MMA to 56.05% with the combined treatment of MAN and MMA [34].

Table 1. Weight percentage gain, volume bulking efficiency, and conversion rate of treated bamboo.

Samples	Weight Percentage Gain (%)	Volume Bulking Efficiency (%)	Conversion Rate (%)
VA-B	11.09 ± 0.56	4.25 ± 0.21	/
MMA-B	6.59 ± 0.33	3.49 ± 0.17	8.68 ± 0.43
VA/MMA-B	18.95 ± 0.95	8.66 ± 0.43	20.69 ± 1.03

Among the three chemical modification methods, the lowest value of VBE was obtained after MMA treatment because the majority of MMA entered the voids of cell walls rather than attached onto the surface of bamboo. In addition, the CR of MMA increased from 8.68% after MMA treatment to 20.69% after the combined treatment of VA and MMA, and this indicates that pretreating bamboo with VA was beneficial for increasing the CR of MMA. VA treatment enhanced interactions between the polymer and bamboo matrix, and more MMA filled the cell lumen of bamboo [41,43]. Li et al. reported that maleic anhydride successfully activated poplar through a nucleophilic substitution reaction and that this newly formed carboxyl group might act as a catalyst by providing a certain level of acidity for polymerization.

3.2. Morphology Characterization

Figure 2 shows morphology characterizations of the cross-section and longitudinal section of raw and pretreated bamboo. Compared to the raw bamboo (Figure 2A,B), the starch granules on the surface of the bamboo cells in the cross-section disappeared after VA treatment. Also, the pits on the parenchymal cells in the longitudinal section disappeared after VA treatment (Figure 2C,D), and this is because of the acetylic inflation [25]. Figure 2E,F clearly shows that MMA was in situ polymerized on the surface of the bamboo, and this is indicated by the tiny spherical granules. As seen in Figure 2G,H, more MMA was fabricated on the surface of the bamboo after the combined treatment of VA and MMA than was fabricated with just the VA treatment. In particular, abundant polymers filled most of the pores and pits in the cross-section and longitudinal section. It was expected that the use of VA would lead to penetration and swelling of the cell wall matrix and to a reduction in the number of hydroxyl groups. Pretreating the bamboo with VA could increase the adhesion amount of MMA on bamboo and create a cross-linked copolymer bonded onto the bamboo cell wall [32,34,37].

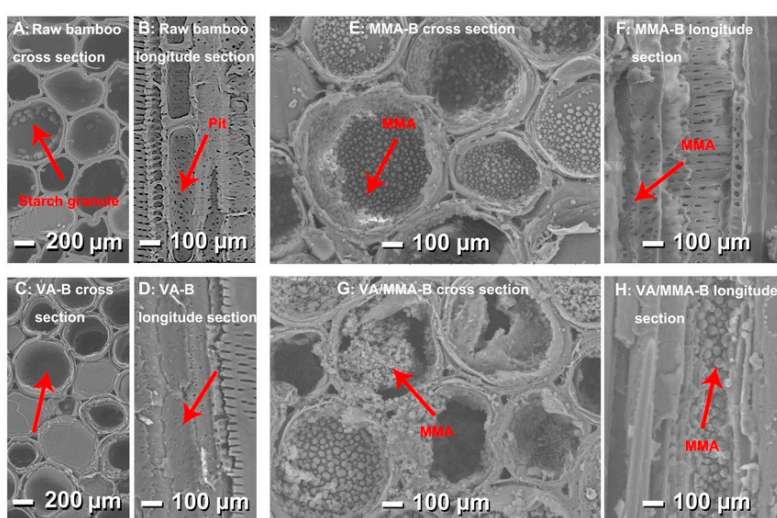


Figure 2. Morphology characterizations of the cross-section and longitudinal section of raw and pretreated bamboo: raw bamboo (A,B), VA-B (C,D), MMA-B (E,F), and VA/MMA-B (G,H).

3.3. FTIR Analysis

Figure 3 shows the effects of chemical modification on the surface functional groups of bamboo. The band at 3405 cm^{-1} is attributed to the stretching vibration of the hydroxyl group [44]. Compared to the spectrum for raw bamboo, the intensity of the hydroxyl group remarkably decreased in the spectrum for the bamboo that was pretreated using VA and MMA. Hydrophilic hydroxyl groups in bamboo are esterified by acetyl groups ($\text{CH}_3\text{CO}-$) in VA, and some of the hydroxyl groups are replaced in the polymer chains during the in situ polymerization process of MMA [37]. Among the three chemical modification methods, the lowest intensity band that corresponded to the hydroxyl group was observed in the spectrum for VA/MMA-B, and this indicates that the dimensional stability of VA/MMA-B was probably better than that of raw bamboo, VA-B, and MMA-B. The band at 2955 cm^{-1} is attributed to the stretching vibration of methyl ($-\text{CH}_3$) and methylene ($-\text{CH}_2-$) [45,46]. Obviously, the intensity of this band in the spectrum of VA/MMA-B is higher than that in the spectra of raw bamboo, MMA-B, and VA-B, and this indicates that more MMA was successfully grafted onto the bamboo cell walls after the combined treatment of VA and MMA [33,40]. The intensity of the band at 1745 cm^{-1} is ascribed to the stretching vibration of carbonyl groups ($\text{C}=\text{O}$) [47]. The intensity of the band for carbonyl groups in the spectrum of VA/MMA-B is much stronger than that in the spectra of raw bamboo and MMA-B, but it is slightly stronger than that in the spectrum of VA-B. This result indicates that quite a number of carbonyl groups from both VA and MMA molecules were grafted onto the bamboo cell walls of VA/MMA-B. Another slightly enhanced peak in the spectrum of VA/MMA-B is the band for the ester bond ($\text{C}-\text{O}$) stretching vibration at 1242 cm^{-1} [46]. This was caused by the successful reaction of bamboo hydroxyl groups with VA and MMA.

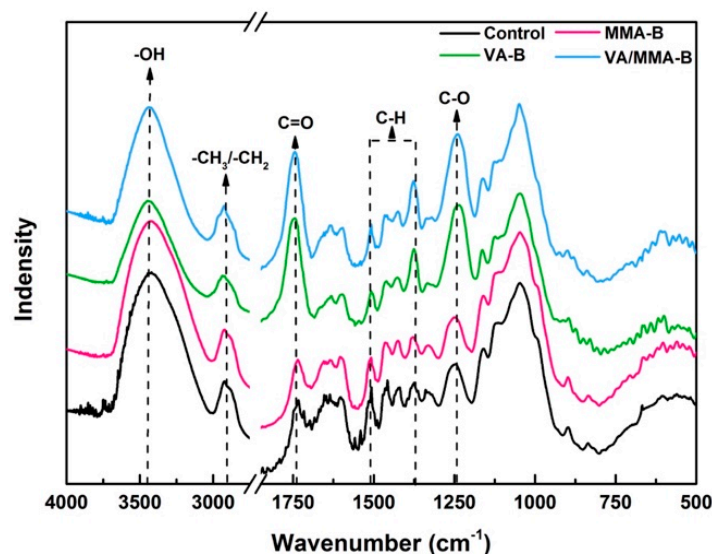


Figure 3. FTIR analysis of raw and pretreated bamboo.

All of the treated bamboo samples were also analyzed using diffuse reflectance FTIR (DRIFT) spectroscopy to study the nonadsorbing matrix. Reflectance spectra were transformed to Kubelka–Munk (K-M) units to minimize scattering contributions to the absorption measured [48,49]. Changes in the relative intensities of bands in the spectra for raw or pretreated bamboo at 1740 cm^{-1} , 1660 cm^{-1} , 1506 cm^{-1} , 1460 cm^{-1} , 1422 cm^{-1} , 1370 cm^{-1} , 1240 cm^{-1} , 1056 cm^{-1} , and 899 cm^{-1} are given in Table 2. These variations in relative intensities of various bands are because of varying quantities of cellulose, hemicellulose, and lignin present in samples that were subjected to different treatments [33,50,51]. The band intensities for VA are always higher than those of the control sample. After MMA polymerization, the bands of VA/MMA-B for the aromatic skeletal vibrations at 1740 cm^{-1} , 1660 cm^{-1} , 1506 cm^{-1} , and 1460 cm^{-1} increased in intensity. Likewise, the intensity of aromatic bending vibration at 1240 and 899 cm^{-1} increased. Regarding single MMA polymerization, the absorptions for C–H were similar

with the raw sample and the band for C–H₂ decreased. The results from DRIFT analysis indicated that acetylation bamboo increased the weight by VA acetylation and also achieved a sufficient chemical complex by MMA polymerization.

Table 2. DRIFT spectra analysis of raw and pretreated bamboo.

Wavenumber/(cm ⁻¹)	Assignment	Peak Height of Associated Bands			
		Control	VA/MMA-B	VA-B	MMA-B
1740	C=O stretching vibration	0.195	0.766	0.494	0.323
1660	H–O–H deformation vibration and conjugated C=O stretching vibration	0.159	0.486	0.440	0.164
1506	Aromatic skeletal	0.171	0.446	0.377	0.171
1460	C–H deformation (asymmetric) and benzene vibration in lignin	0.190	0.421	0.457	0.176
1422	C–H deformation (asymmetric)	0.189	0.457	0.457	0.189
1370	C–H ₂ deformation (symmetric)	0.454	0.530	0.229	0.187
1240	C–O stretching vibration in lignin, acetyl and carboxylic vibration in xylan	0.180	0.587	0.470	0.248
1056	C–O stretching	0.177	0.526	0.472	0.231
899	C1 group frequency in cellulose and hemicellulose	0.077	0.216	0.132	0.065

3.4. Dimensional Stability

Figure 4 shows the effects of chemical modification on the dimensional stability of bamboo in the three cycles of water soaking–drying experiments. Figure 4 includes data for the volume swelling ratio, volume shrinkage ratio, antismelling efficiency, and water absorption. Compared to control samples, the volume swelling ratio and volume shrinkage ratio of bamboo treated using the three chemical modification methods all decreased, and this indicates that the dimensional stability of bamboo treated using VA and MMA was improved. Among the three chemical modification methods, bamboo treated with the combination of VA and MMA exhibited the best dimensional stability. The antismelling efficiency of VA/MMA-B reached a maximum value of 40.71%. We suggested that VA reacts with and deactivates the hygroscopic hydroxyl groups of the cell wall polymers and thereby creates a less polar particle surface, which is for better polymerization [30,34,40].

As reported in the literature, the hydrophilic hydroxyl groups are esterified by acetyl groups (CH₃CO–) in VA, and this leads to a decreased availability of sites for hydrogen bonding. Furthermore, the voids of bamboo cell lumen are physically blocked via in situ polymerization of MMA, and this hinders the interaction between hydrophilic hydroxyl groups in bamboo and water in the environment [30,31,37]. With an increase in the number of times that the water soaking–drying experiment was repeated, the dimensional stability of bamboo that was treated using the three chemical modification methods decreased. This resulted in an increase in water absorption, as seen in Figure 4d. This observation is explained by the fact that part of the covering layer that formed between the bamboo surface and VA/MMA might be destroyed in the process of several rounds of the water soaking–drying experiment. A reason for this may be the partial loss of the polymer and a high physical cross-linking ratio for the treated samples during the water soaking–drying process. According to Li et al., the ASE of Poplar–PMGM–C also decreased after the third water immersion, and this is the same as our results [43]. Moreover, Zhang et al. indicated that the formed polymer also has a certain water absorption and hygroscopicity because of the high water absorption of the MMA monomer, and this may clarify our observation as well [36].

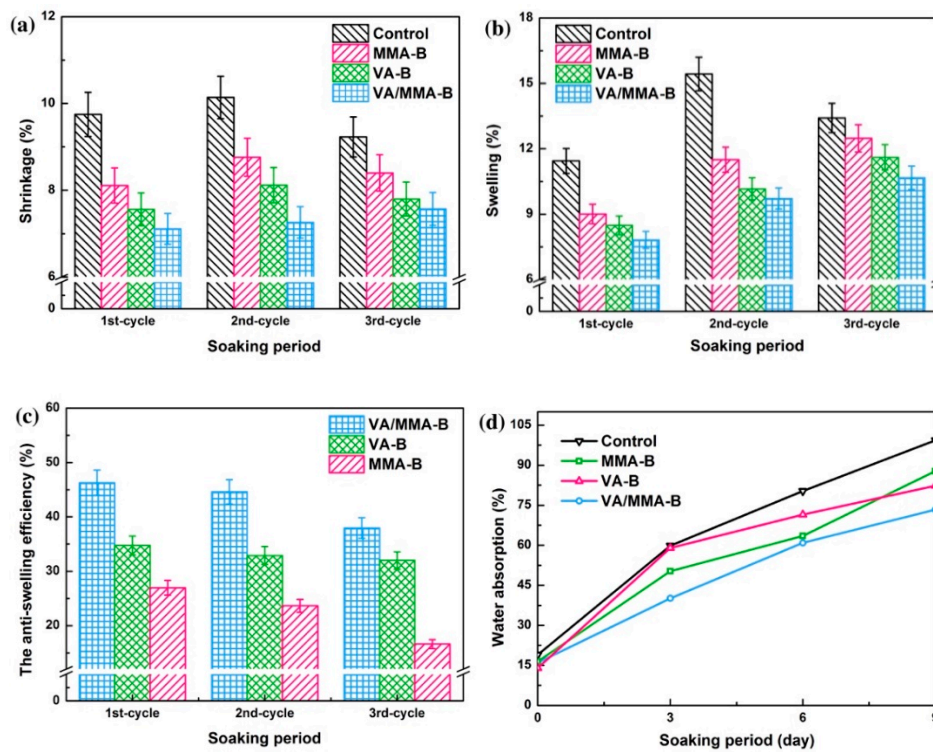


Figure 4. Dimensional stability of bamboo after different chemical modifications with three cycles of water soaking–drying experiments: volume shrinkage ratio (a), volume swelling ratio (b), anti-swelling efficiency (c), and water absorption (d).

3.5. Wettability Analysis

The wettability of raw and pretreated bamboo was evaluated using contact angle analysis (CA), where a large contact angle corresponds to greater hydrophobicity and better dimensional stability [52]. Figure 5 shows the transient profiles of the CA data of raw and pretreated bamboo. For the untreated samples, the initial CA was 94.3°, and then it sharply dropped to 28.5° with an increase in contact time from 1 s to 5 s. After chemical modification, the CA values of VA-B, MMA-B, and VA/MMA-B were 93.3–43.3°, 90.7–65.2°, and 107.1–84.9°, respectively, with varying contact times. Similar to CA data for raw bamboo, the CAs of treated bamboo gradually decreased with an increase in contact time. This result might have been caused by the surface defects of bamboo, where VA and MMA were not uniformly distributed. This defect makes it hard to obtain Young’s equilibrium CA, and the static CA might fluctuate within a range under real conditions [53].

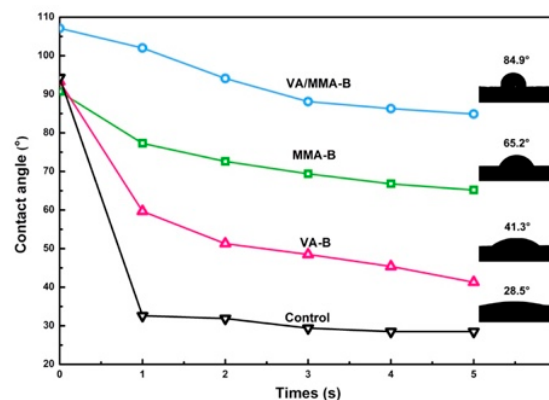


Figure 5. Contact angle profiles for the surfaces of raw and pretreated bamboo.

Among the three chemical modification methods, VA/MMA-B had the highest CA value of 84.9–107.1°, indicating that VA/MMA-B had the greatest hydrophobicity and best dimensional stability. The hydrophilic functional groups were greatly reduced by VA acetylation and in situ polymerization of MMA [23,43]. This result indicates that the combined treatment of VA and MMA is an efficient method for improving the dimensional stability and polymer coverage of the bamboo surface [39].

3.6. TG Analysis

Figure 6 shows the thermal degradation behaviors of raw and pretreated bamboo under a nitrogen atmosphere at a heating rate of 10 °C/min. According to the TG curves, the highest residual mass was observed in raw bamboo (24.5%), followed by MMA-B (21.4%), VA-B (21.3%), and VA/MMA-B (20.4%). The thermal stability of VA and MMA was lower than that of raw bamboo. Therefore, with an increase in the WPG of treated bamboo, the residual mass decreased, but the weight loss rate of the treated bamboo increased.

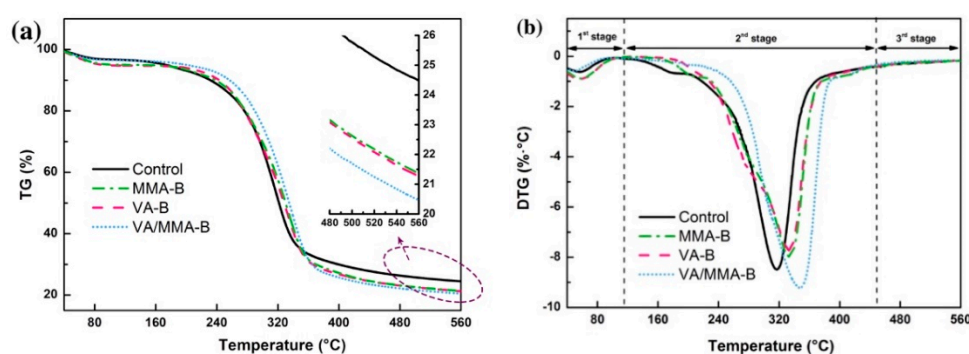


Figure 6. Thermal degradation behaviors of raw and pretreated bamboo: TG (a) and DTG (b) curves.

According to the DTG curves, the thermal degradation process of bamboo can be divided into three stages: the moisture evaporation stage (50–150 °C), fast devolatilization stage (150–450 °C), and carbonization stage (450–650 °C) [44,46,54–56]. In the fast devolatilization stage, the peak temperatures of the maximum weight loss for raw bamboo, MMA-B, VA-B, and VA/MMA-B were 317 °C, 334 °C, 333 °C, and 337 °C, respectively. This gradually moved toward the side of higher pyrolysis temperature with an increase in the extent of pretreatment via the chemical modifications. This result indicates that VA/MMA-B had enhanced thermal stability compared to all of the other samples. The esterification reaction between VA and the hydroxy groups in bamboo resulted in an increase in the degree of the crystallinity of cellulose, and this was in good agreement with the results from Wei et al. [51]. The decrease in residual mass after grafting MMA was because of the presence of MMA, which degraded more easily than bamboo [42].

3.7. Dynamic Mechanical Analysis

Variations in the dynamic storage modulus (E'), loss modulus (E''), and loss tangent ($\tan \delta$) of raw and pretreated bamboo are shown in Figure 7. The dynamic storage modulus is widely used to assess the load-bearing capability of a composite material [57]. The storage modulus of raw bamboo was about 15,057 Pa. In general, the storage modulus (E') of all of the bamboo samples decreased with an increase in temperature. It is worth noting that the value of E' for VA/MMA-B was the highest at the same temperature for each of the four samples (17,909 Pa), and this indicates that the dynamic storage modulus was enhanced after the combined pretreatment using VA and MMA. With an increase in the concentration of acetyl and methyl groups, intermolecular hydrogen bonding was broken. A certain number of hydroxyl groups were then regenerated, and the cellulose chains were consequently closer [32,33,41]. It is believed that the stiffness of the bamboo fibers was enhanced, and the initial storage modulus value of the treated samples is also reflected by this. A similar result has been reported

by Jebrane et al. Some esterified material expands into the micropores or lumen of the bamboo cell wall after treatment, and this results in a higher value of E' [23].

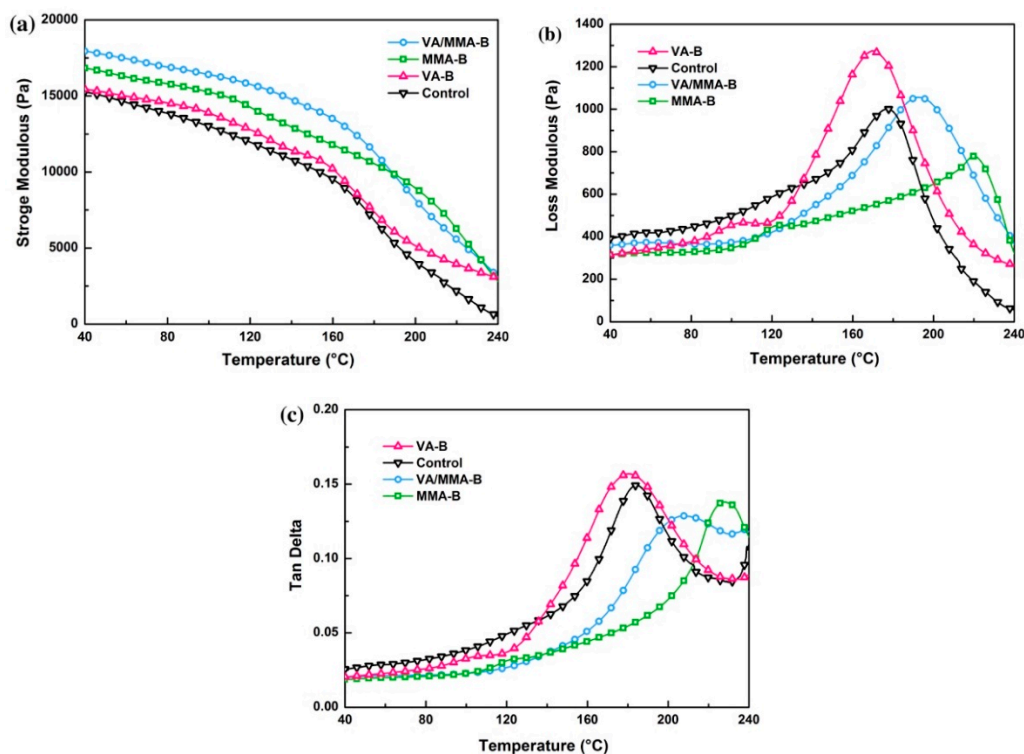


Figure 7. Storage modulus (E') (a), loss modulus (E'') (b), and loss tangent ($\tan \delta$) (c) curves of raw and treated bamboo.

Figure 7b illustrates the temperature spectrum of the loss modulus (E'') for raw and pretreated bamboo over the entire temperature range. The highest value of E'' was obtained for VA-B (1275.4 Pa at 170 °C), and the lowest value was for MMA-B (785.5 Pa at 220 °C). With an increase in the in situ polymerization of MMA on bamboo, intermolecular friction and energy consumption of bamboo also increased. Furthermore, a decrease in E'' is consistent with some internal plasticization occurring after polymerization, and this causes a decrease in the energy required to initiate chain mobility [58]. Researchers have reported that the thermal-softening temperature of lignin, hemicellulose, and cellulose are 30–205 °C, 150–220 °C, and 200–250 °C, respectively [59,60]. The loss peak at a temperature of 200 °C is labeled as an α relaxation process that is derived from micro-Brownian motions of bamboo cell wall polymers in the noncrystalline region [28,59]. After chemical modification, there was a remarkable difference in the α relaxation process for different samples. Compared to raw bamboo, the in situ polymerization of MMA on bamboo (MMA-B and VA/MMA-B) led to higher temperature of the α -peak because more MMA, which has amorphous chains, was grafted onto the bamboo. However, acetylation with VA did not significantly influence the temperature of the α -peak.

Figure 7c shows the glass transition temperature for raw and pretreated bamboo in terms of the mechanical loss factor ($\tan \delta$). The glass transition temperature (T_g) was approximately equal to the temperature when $\tan \delta$ reached its maximum value. After in situ polymerization of MMA on bamboo, the glass transition temperature increased from 180 °C for raw bamboo to 205 °C for VA/MMA-B and 220 °C for MMA-B. The increased glass transition temperature should be ascribed to the reinforcement of polymer on bamboo as caused by the in situ polymerization of MMA in cell lumen [33]. However, compared to the glass transition temperature for raw bamboo, a slight decrease was observed in the glass transition temperature for VA-B (175 °C).

4. Conclusions

The effects of the combined treatment with VA and MMA on dimensional stability, chemical structure, and dynamic mechanical properties of bamboo were systematically investigated. Results show that the dimensional stability (i.e., antiswelling efficiency and water absorption) of bamboo after the combined treatment of VA and MMA was remarkably improved because of the decrease in hydrophilic hydroxyl groups. VA and MMA were mainly grafted onto the surface of the cell walls or in the bamboo cell lumen. From TG analysis, an increase in the extent of pretreatment via chemical modifications resulted in the peak temperatures of the maximum weight loss gradually moving toward the side of higher pyrolysis temperature. From DMA analysis, compared to untreated and single-treated bamboo, the storage modulus (E') of VA/MMA-B sharply increased by about 3 MPa, and the glass transition temperature increased from 180 °C to 205 °C. At the same time, the glass transition temperature of MMA-B was the highest (220 °C).

Author Contributions: Conceptualization and experiment design was done by Z.M. and L.M.; material preparation and methodology were done by S.H., Q.J., B.Y., and Y.N.; software was done by S.H. and Q.J.; review and editing were done by Z.M. and L.M.; data analysis and discussion were done by all of the authors.

Funding: This research was funded by the Natural Science Foundation of China (31270592), the Fund of Zhejiang Provincial Collaborative Innovation Center for Bamboo Resources and High-Efficiency Utilization (2017ZZY2-02), and the Young Elite Scientists Sponsorship Program by CAST (2018QNR001).

Conflicts of Interest: The authors declare no conflict of interest.

References

1. Yeasmin, L.; Ali, M.N.; Gantait, S.; Chakraborty, S. Bamboo: An overview on its genetic diversity and characterization. *3 Biotech* **2015**, *5*, 1–11. [[CrossRef](#)] [[PubMed](#)]
2. Archila, H.; Kaminski, S.; Trujillo, D.; Zea Escamilla, E.; Harries, K.A. Bamboo reinforced concrete: A critical review. *Mater. Struct.* **2018**, *51*, 102. [[CrossRef](#)]
3. Bekhta, P.; Niemz, P. Effect of high temperature on the change in color, dimensional stability and mechanical properties of spruce wood. *Holzforschung* **2003**, *57*, 539–546. [[CrossRef](#)]
4. Hakkou, M.; Pétrissans, M.; Zoulalian, A.; Gérardin, P. Investigation of wood wettability changes during heat treatment on the basis of chemical analysis. *Polym. Degrad. Stab.* **2005**, *89*, 1–5. [[CrossRef](#)]
5. Rowell, R.M.; Ibach, R.E.; McSweeney, J.; Nilsson, T. Understanding decay resistance, dimensional stability and strength changes in heat-treated and acetylated wood. *Wood Mater. Sci. Eng.* **2009**, *4*, 14–22. [[CrossRef](#)]
6. He, Z.; Qu, L.; Wang, Z.; Qian, J.; Yi, S. Effects of zinc chloride–silicone oil treatment on wood dimensional stability, chemical components, thermal decomposition and its mechanism. *Sci. Rep.* **2019**, *9*, 1601. [[CrossRef](#)] [[PubMed](#)]
7. Bhaskar, J.; Haq, S.; Yadaw, S.B. Evaluation and testing of mechanical properties of wood plastic composite. *J. Thermoplast. Compos. Mater.* **2011**, *25*, 391–401. [[CrossRef](#)]
8. Krehula, L.K.; Katančić, Z.; Siročić, A.P.; Hrnjak-Murgić, Z. Weathering of high-density polyethylene-wood plastic composites. *J. Wood Chem. Technol.* **2013**, *34*, 39–54. [[CrossRef](#)]
9. Seki, M.; Tanaka, S.; Miki, T.; Shigematsu, I.; Kanayama, K. Forward extrusion of bulk wood containing polymethylmethacrylate: Effect of polymer content and die angle on the flow characteristics. *J. Mater. Process. Technol.* **2017**, *239*, 140–146. [[CrossRef](#)]
10. Hung, K.-C.; Wu, T.-L.; Chen, Y.-L.; Wu, J.-H. Assessing the effect of wood acetylation on mechanical properties and extended creep behavior of wood/recycled-polypropylene composites. *Constr. Build. Mater.* **2016**, *108*, 139–145. [[CrossRef](#)]
11. Kumar, S. Chemical modification of wood. *Wood Fiber Sci.* **2007**, *26*, 270–280.
12. Kurimoto, Y.; Sasaki, S. Preparation of acetylated wood meal and polypropylene composites ii: Mechanical properties and dimensional stability of the composites. *J. Wood Sci.* **2013**, *59*, 216–220. [[CrossRef](#)]
13. Rowell, R.M. 14 chemical modification of wood. In *Handbook of Wood Chemistry and Wood Composites*; CRC Press: Boca Raton, FL, USA, 2005; pp. 381–413.

14. Xie, Y.; Krause, A.; Militz, H.; Turkulin, H.; Richter, K.; Mai, C. Effect of treatments with 1,3-dimethylol-4,5-dihydroxy-ethyleneurea (dmdheu) on the tensile properties of wood. *Holzforschung* **2007**, *61*, 43–50. [[CrossRef](#)]
15. Xie, Y.; Xiao, Z.; Grüneberg, T.; Militz, H.; Hill, C.A.S.; Steuernagel, L.; Mai, C. Effects of chemical modification of wood particles with glutaraldehyde and 1,3-dimethylol-4,5-dihydroxyethyleneurea on properties of the resulting polypropylene composites. *Compos. Sci. Technol.* **2010**, *70*, 2003–2011. [[CrossRef](#)]
16. Jiang, T.; Gao, H.; Sun, J.; Xie, Y.; Li, X. Impact of dmdheu resin treatment on the mechanical properties of poplar. *Polym. Polym. Compos.* **2014**, *22*, 669–674. [[CrossRef](#)]
17. Rowell, R.M.; Simonson, R.; Hess, S.; Plackett, D.V.; Cronshaw, D.; Dunningham, E. Acetyl distribution in acetylated whole wood and reactivity of isolated wood cell-wall components to acetic anhydride. *Wood Fiber Sci.* **2007**, *26*, 11–18.
18. Obataya, E.; Furuta, Y.; Gril, J. Dynamic viscoelastic properties of wood acetylated with acetic anhydride solution of glucose pentaacetate. *J. Wood Sci.* **2003**, *49*, 152–157. [[CrossRef](#)]
19. Kumari, R.; Ito, H.; Takatani, M.; Uchiyama, M.; Okamoto, T. Fundamental studies on wood/cellulose-plastic composites: Effects of composition and cellulose dimension on the properties of cellulose/pp composite. *J. Wood Sci.* **2007**, *53*, 470–480. [[CrossRef](#)]
20. Li, J.; Zhang, L.-P.; Peng, F.; Bian, J.; Yuan, T.-Q.; Xu, F.; Sun, R.-C. Microwave-assisted solvent-free acetylation of cellulose with acetic anhydride in the presence of iodine as a catalyst. *Molecules* **2009**, *14*, 3551–3566. [[CrossRef](#)]
21. Huang, X.; Kocaefe, D.; Kocaefe, Y.; Pichette, A. Combined effect of acetylation and heat treatment on the physical, mechanical and biological behavior of jack pine (*pinus banksiana*) wood. *Eur. J. Wood Wood Prod.* **2017**, *76*, 525–540. [[CrossRef](#)]
22. Hill, C.A.S.; Jones, D.; Strickland, G.; Cetin, N.S. Kinetic and mechanistic aspects of the acetylation of wood with acetic anhydride. *Holzforschung* **1998**, *52*, 623–629. [[CrossRef](#)]
23. Jebrane, M.; Sèbe, G. A novel simple route to wood acetylation by transesterification with vinyl acetate. *Holzforschung* **2007**, *61*, 143–147. [[CrossRef](#)]
24. Huang, S.; Ma, Z.; Nie, Y.; Lu, F.; Ma, L. Comparative study of the performance of acetylated bamboo with different catalysts. *BioResources* **2018**, *14*, 44–58.
25. Li, J.-Z.; Furuno, T.; Katoh, S.; Uehara, T. Chemical modification of wood by anhydrides without solvents or catalysts. *J. Wood Sci.* **2000**, *46*, 215–221. [[CrossRef](#)]
26. Hill, C. Modifying the properties of wood. In *Wood Modification: Chemical, Thermal and Other Processes*; Wiley: Hoboken, NJ, USA, 2006; pp. 19–44.
27. Çetin, N.S.; Özmen, N.; Birinci, E. Acetylation of wood with various catalysts. *J. Wood Chem. Technol.* **2011**, *31*, 142–153. [[CrossRef](#)]
28. Jebrane, M.; Harper, D.; Labbé, N.; Sèbe, G. Comparative determination of the grafting distribution and viscoelastic properties of wood blocks acetylated by vinyl acetate or acetic anhydride. *Carbohydr. Polym.* **2011**, *84*, 1314–1320. [[CrossRef](#)]
29. Jebrane, M.; Pichavant, F.; Sèbe, G. A comparative study on the acetylation of wood by reaction with vinyl acetate and acetic anhydride. *Carbohydr. Polym.* **2011**, *83*, 339–345. [[CrossRef](#)]
30. Özmen, N.; Çetin, N.S.; Mengeloğlu, F.; Birinci, E.; Karakuş, K. Effect of wood acetylation with vinyl acetate and acetic anhydride on the properties of wood-plastic composites. *BioResources* **2013**, *8*, 753–767. [[CrossRef](#)]
31. Huang, J.; Schols, H.A.; Jin, Z.; Sulmann, E.; Voragen, A.G. Characterization of differently sized granule fractions of yellow pea, cowpea and chickpea starches after modification with acetic anhydride and vinyl acetate. *Carbohydr. Polym.* **2007**, *67*, 11–20. [[CrossRef](#)]
32. Cetin, N.S.; Tingaut, P.; Özmen, N.; Henry, N.; Harper, D.; Dadmun, M.; Sebe, G. Acetylation of cellulose nanowhiskers with vinyl acetate under moderate conditions. *Macromol. Biosci.* **2009**, *9*, 997–1003. [[CrossRef](#)] [[PubMed](#)]
33. YongFeng, L.; XiaoYing, D.; ZeGuang, L.; WanDa, J.; YiXing, L. Effect of polymer in situ synthesized from methyl methacrylate and styrene on the morphology, thermal behavior, and durability of wood. *J. Appl. Polym. Sci.* **2013**, *128*, 13–20. [[CrossRef](#)]
34. Ghorbani, M.; Nikkha Shahmirzadi, A.; Amininasab, S.M. Physical and morphological properties of combined treated wood polymer composites by maleic anhydride and methyl methacrylate. *J. Wood Chem. Technol.* **2017**, *37*, 443–450. [[CrossRef](#)]

35. Yildiz, Ü.C.; Yildiz, S.; Gezer, E.D. Mechanical properties and decay resistance of wood–polymer composites prepared from fast growing species in turkey. *Bioresour. Technol.* **2005**, *96*, 1003–1011. [[CrossRef](#)] [[PubMed](#)]
36. Zhang, Y.; Zhang, S.Y.; Yang, D.Q.; Wan, H. Dimensional stability of wood–polymer composites. *J. Appl. Polym. Sci.* **2006**, *102*, 5085–5094. [[CrossRef](#)]
37. Mattos, B.D.; de Cademartori, P.H.; Missio, A.L.; Gatto, D.A.; Magalhães, W.L. Wood-polymer composites prepared by free radical in situ polymerization of methacrylate monomers into fast-growing pinewood. *Wood Sci. Technol.* **2015**, *49*, 1281–1294. [[CrossRef](#)]
38. Shang, L.; Jiang, Z.; Tian, G.; Ma, J.; Yang, S. Effect of modification with methyl methacrylate on the mechanical properties of plectocomia kerrana rattan. *Bioresources* **2016**, *11*, 2071–2082. [[CrossRef](#)]
39. Fu, Y.; Li, G.; Yu, H.; Liu, Y. Hydrophobic modification of wood via surface-initiated arget atrp of mma. *Appl. Surf. Sci.* **2012**, *258*, 2529–2533. [[CrossRef](#)]
40. Yu, F.; Yang, W.; Song, J.; Wu, Q.; Chen, L. Investigation on hydrophobic modification of bamboo flour surface by means of atom transfer radical polymerization method. *Wood Sci. Technol.* **2013**, *48*, 289–299. [[CrossRef](#)]
41. Li, Y.F.; Liu, Y.X.; Wang, X.M.; Wu, Q.L.; Yu, H.P.; Li, J. Wood–polymer composites prepared by the in situ polymerization of monomers within wood. *J. Appl. Polym. Sci.* **2011**, *119*, 3207–3216. [[CrossRef](#)]
42. Stolf, D.O.; Bertolini, M.d.S.; Christoforo, A.L.; Panzera, T.H.; Ribeiro Filho, S.L.M.; Lahr, F.A.R. Pinus caribaeavar. Hondurensis wood impregnated with methyl methacrylate. *J. Mater. Civ. Eng.* **2017**, *29*, 05016004. [[CrossRef](#)]
43. Li, Y.; Wu, Q.; Li, J.; Liu, Y.; Wang, X.-M.; Liu, Z. Improvement of dimensional stability of wood via combination treatment: Swelling with maleic anhydride and grafting with glycidyl methacrylate and methyl methacrylate. *Holzforschung* **2012**, *66*, 59–66. [[CrossRef](#)]
44. Ma, Z.; Wang, J.; Li, C.; Yang, Y.; Liu, X.; Zhao, C.; Chen, D. New sight on the lignin torrefaction pretreatment: Relevance between the evolution of chemical structure and the properties of torrefied gaseous, liquid, and solid products. *Bioresour. Technol.* **2019**, *288*, 121528. [[CrossRef](#)] [[PubMed](#)]
45. Ma, Z.; Chen, D.; Gu, J.; Bao, B.; Zhang, Q. Determination of pyrolysis characteristics and kinetics of palm kernel shell using tga–ftir and model-free integral methods. *Energy Convers. Manag.* **2015**, *89*, 251–259. [[CrossRef](#)]
46. Chen, D.; Wang, Y.; Liu, Y.; Cen, K.; Cao, X.; Ma, Z.; Li, Y. Comparative study on the pyrolysis behaviors of rice straw under different washing pretreatments of water, acid solution, and aqueous phase bio-oil by using tg-ftir and py-gc/ms. *Fuel* **2019**, *252*, 1–9. [[CrossRef](#)]
47. Ma, Z.; Zhang, Y.; Li, C.; Yang, Y.; Zhang, W.; Zhao, C.; Wang, S. N-doping of biomass by ammonia (nh₃) torrefaction pretreatment for the production of renewable n-containing chemicals by fast pyrolysis. *Bioresour. Technol.* **2019**, *292*, 122034. [[CrossRef](#)] [[PubMed](#)]
48. Zeng, Y.; Yang, X.; Yu, H.; Zhang, X.; Ma, F. The delignification effects of white-rot fungal pretreatment on thermal characteristics of moso bamboo. *Bioresour. Technol.* **2012**, *114*, 437–442. [[CrossRef](#)] [[PubMed](#)]
49. Nuopponen, M.H.; Birch, G.M.; Sykes, R.J.; Lee, S.J.; Stewart, D. Estimation of wood density and chemical composition by means of diffuse reflectance mid-infrared fourier transform (drift-mir) spectroscopy. *J. Agric. Food Chem.* **2006**, *54*, 34–40. [[CrossRef](#)] [[PubMed](#)]
50. Weiland, J.-J.; Guyonnet, R. Study of chemical modifications and fungi degradation of thermally modified wood using drift spectroscopy. *Holz Als Roh-Und Werkst.* **2003**, *61*, 216–220. [[CrossRef](#)]
51. Ye, X.; Wang, H.; Wu, Z.; Zhou, H.; Tian, X. The functional features and interface design of wood/polypropylene composites based on microencapsulated wood particles via adopting in situ emulsion polymerization. *Polym. Compos.* **2018**, *39*, 427–436. [[CrossRef](#)]
52. Xu, J.; Zhang, Y.; Shen, Y.; Li, C.; Wang, Y.; Ma, Z.; Sun, W. New perspective on wood thermal modification: Relevance between the evolution of chemical structure and physical-mechanical properties, and online analysis of release of vocs. *Polymers* **2019**, *11*, 1145. [[CrossRef](#)]
53. Nystrom, D.; Lindqvist, J.; Ostmark, E.; Antoni, P.; Carlmark, A.; Hult, A.; Malmstrom, E. Superhydrophobic and self-cleaning bio-fiber surfaces via atrp and subsequent postfunctionalization. *ACS Appl. Mater. Interfaces* **2009**, *1*, 816–823. [[CrossRef](#)]
54. Chen, Y.; Liu, B.; Yang, H.; Wang, X.; Zhang, X.; Chen, H. Generalized two-dimensional correlation infrared spectroscopy to reveal the mechanisms of lignocellulosic biomass pyrolysis. *Proc. Combust. Inst.* **2019**, *37*, 3013–3021. [[CrossRef](#)]

55. Ma, Z.; Zhang, Y.; Shen, Y.; Wang, J.; Yang, Y.; Zhang, W.; Wang, S. Oxygen migration characteristics during bamboo torrefaction process based on the properties of torrefied solid, gaseous, and liquid products. *Biomass Bioenergy* **2019**, *128*, 105300. [[CrossRef](#)]
56. Ma, Z.; Wang, J.; Zhou, H.; Zhang, Y.; Yang, Y.; Liu, X.; Ye, J.; Chen, D.; Wang, S. Relationship of thermal degradation behavior and chemical structure of lignin isolated from palm kernel shell under different process severities. *Fuel Process. Technol.* **2018**, *181*, 142–156. [[CrossRef](#)]
57. Das, M.; Chakraborty, D. Influence of mercerization on the dynamic mechanical properties of bamboo, a natural lignocellulosic composite. *Ind. Eng. Chem. Res.* **2006**, *45*, 6489–6492. [[CrossRef](#)]
58. Su, C.; Zong, D.; Xu, L.; Zhang, C. Dynamic mechanical properties of semi-interpenetrating polymer network-based on nitrile rubber and poly (methyl methacrylate-co-butyl acrylate). *J. Appl. Polym. Sci.* **2014**, *131*, 40217. [[CrossRef](#)]
59. Jiang, J.; Lu, J. Dynamic viscoelastic behavior of wood under drying conditions. *Front. For. China* **2009**, *4*, 374–379. [[CrossRef](#)]
60. Hristov, V.; Vasileva, S. Dynamic mechanical and thermal properties of modified poly (propylene) wood fiber composites. *Macromol. Mater. Eng.* **2003**, *288*, 798–806. [[CrossRef](#)]



© 2019 by the authors. Licensee MDPI, Basel, Switzerland. This article is an open access article distributed under the terms and conditions of the Creative Commons Attribution (CC BY) license (<http://creativecommons.org/licenses/by/4.0/>).